Green Chemistry

PAPER

View Article Online
View Journal | View Issue

Cite this: *Green Chem.*, 2022, **24**, 6016

1,2,3-Trimethoxypropane: a bio-sourced glyme as electrolyte for lithium–O_2 batteries†

Marta Alvarez-Tirado, [a,b] Laurent Castro,*[b] Shuai Qian,[c] Jason E. Bara, [c] Marco Di Gennaro,[d] Konstantinos Gkagkas, [b] Aurélie Guéguen[b] and David Mecerreyes *[a,e]

Li–O_2 batteries are actively being investigated due to their high theoretical energy density (~11 000 Wh kg^{-1}), which would compete with gasoline energy per Kg in electric vehicles. Linear glymes are the most appealing electrolytes for Li–O_2 batteries due to their large electrochemical window, stability against radicals and solubility of Li^+ metal ions. However, all these superior properties are tarnished by their high toxicity. Herein, a greener glyme derived from bio-sourced glycerol (1,2,3-trimethoxypropane (TMP)), is proposed for the first time as a solvent in an electrolyte for Li–O_2 batteries. TMP performance has been compared to its toxic linear isomer, diglyme, and most popular tetraglyme as a liquid electrolyte and gel polymer electrolyte (GPE) membranes. GPEs were based on a mix of mono-, di- and tri- functional acrylates, cured simultaneously within a liquid electrolyte mix (1 M LiTFSI in the plasticizers) by UV-photopolymerisation. GPE-TMP based membranes showed a high ionic conductivity (2.33×10^{-3} S cm^{-1} at 25 °C), directly comparable to the other glymes. Moreover, this remarkable conductivity was very close to the liquid TMP-based electrolyte (3.59×10^{-3} S cm^{-1} at 25 °C). When used as electrolytes in lithium symmetrical cells, the GPE-TMP electrolyte enhanced the polarisation when compared to the liquid TMP-based cells, especially at higher rates (<0.6 V observed at ±1 mA cm^{-2}). Performance in Li–O_2 cells showed that GPE-TMP electrolytes achieved a discharge capacity as high as 2.75 mA h cm^{-2} (3819 mA h g^{-1}), ahead of GPE-diglyme or GPE-tetraglyme electrolytes (2.34 and 2.09 mA h cm^{-2}, respectively). When cycled, cells using TMP-based electrolyte had a similar capacity retention than the ones with tetraglyme, confirming the potential use of TMP as solvent/plasticizer in electrolytes for Li–O_2 cells.

Received 26th April 2022,
Accepted 16th July 2022

DOI: 10.1039/d2gc01567f

rsc.li/greenchem

Introduction

It is clear that lithium-ion batteries (LIBs) are a key enabler technology in terms of electrifying road transport.[1] However, materials resourcing and global demand is forcing the research community to look into other battery chemistries that are more sustainable (*e.g.* batteries based on naturally abundant elements) and efficient (*e.g.* higher energy densities).[2,3]

Beyond LIBs, Li–O_2 batteries have been investigated for a long period of time due to their huge potential (theoretical energy density of ~11 000 Wh kg^{-1}).[4] However, practical deployment is still limited by difficult challenges such as the resistance to degradation of the electrolyte against the oxo-radicals (O_2^-), limited rate capability (1–2 orders of magnitude below LIBs); or the growth of lithium dendrites at the lithium surface.[5,6] Regarding materials for Li–O_2 batteries, glyme-based liquid electrolytes (also known as glycol diethers, glymes are saturated polyethers containing no other functional groups)[7] usually show the best performance. Amongst them, tetraethylene glycol dimethyl ether (G4, tetraglyme) is, perhaps, the most popular one due to its wide electrochemical window, low volatility (requirement for the open-to-air cells) and good solubility of alkali metal ions (*i.e.*, Li^+).[5,8,9] However, this aprotic solvent comes from petroleum-based sources[7] and it is highly toxic for the environment and humans, with important health hazards related to reproductive toxicity (Table S1†).

In 2013, Lemaire and co-workers[10] developed an efficient etherification of glycerol, leading to the synthesis of a bio-sourced branched glyme: 1,2,3-trimethoxypropane (TMP).

[a]*POLYMAT University of the Basque Country UPV/EHU, Avenida Tolosa 72, Donostia-San Sebastian 2008, Spain*
[b]*Material Engineering Division, Toyota Motor Europe NV/SA, Technical Center, 1930 Zaventem, Belgium*
[c]*Department of Chemical & Biological Engineering, University of Alabama, Box 870203, Tuscaloosa, Alabama 35487-0203, USA*
[d]*Nanomat, Q-Mat, CESAM, European Theoretical Spectroscopy Facility, Universite de Liege, B-4000 Liege, Belgium*
[e]*Ikerbasque, Basque Foundation for Science, E-48011 Bilbao, Spain*

† Electronic supplementary information (ESI) available: Solvent properties, simulation details, solvent synthesis details, FT-IR, TGA, ionic conductivity, DMTA, EIS, ramp test, galvanostatic cycling, XRD. See DOI: https://doi.org/10.1039/d2gc01567f

According to several researches,[11,12] TMP was found to have no dermal irritation, no mutagenic activity or no acute toxicity; furthermore, it was added to the *GSK Solvent Sustainability Guide.*[13] It is worth noting that, although these studies revealed encouraging preliminary results regarding its toxicity, TMP has not been legally regulated yet and its full hazards need to be carefully analyzed. Curiously, TMP is a constitutional isomer of the highly toxic linear tri-ether diethylene glycol dimethyl ether (G2, diglyme) (Fig. 1a), which is also a very well-known efficient aprotic solvent candidate in electrolytes for Li–O_2 applications.[14,15] Since TMP was first synthetized, dissimilar applications have been sought for this solvent, such as oxygenated bio-sourced additive for fuels,[16,17] as solvent for the reduction of organic functions[11] or CO_2 capture.[12] In this last publication, Bara *et al.* highlighted the thermophysical properties of TMP and suggested the potential of this molecule for the solvation of metal cations such as Li^+, as confirmed later by preliminary Molecular Dynamics (MD) simulations.[18] However, to the best of our knowledge TMP has not been investigated as electrolyte in lithium batteries.

In this work, we evaluate for the first time the potential of TMP, a low toxicity and greener ether-based solvent, to be used in an electrolyte for Li–O_2 batteries. Furthermore, and beyond liquid electrolyte-based cells, we also propose a solid gel polymer electrolyte (GPE) to improve safety in the battery by avoiding leaking of the liquid electrolyte.[19] GPEs were prepared using a fast and green UV-photopolymerization method by combining a polymer matrix and a conducting Li + salt dissolved in TMP, which acts as a plasticizer (*i.e.*, liquid electrolyte). The key properties of GPEs such as high ionic conductivity, compatibility with lithium metal, good flexibility and solid-like mechanical stability were investigated.[20,21] As a final application, the TMP-based liquid and GPE electrolytes were characterized and tested in lithium symmetrical cells as well as in lithium–O_2 cells.

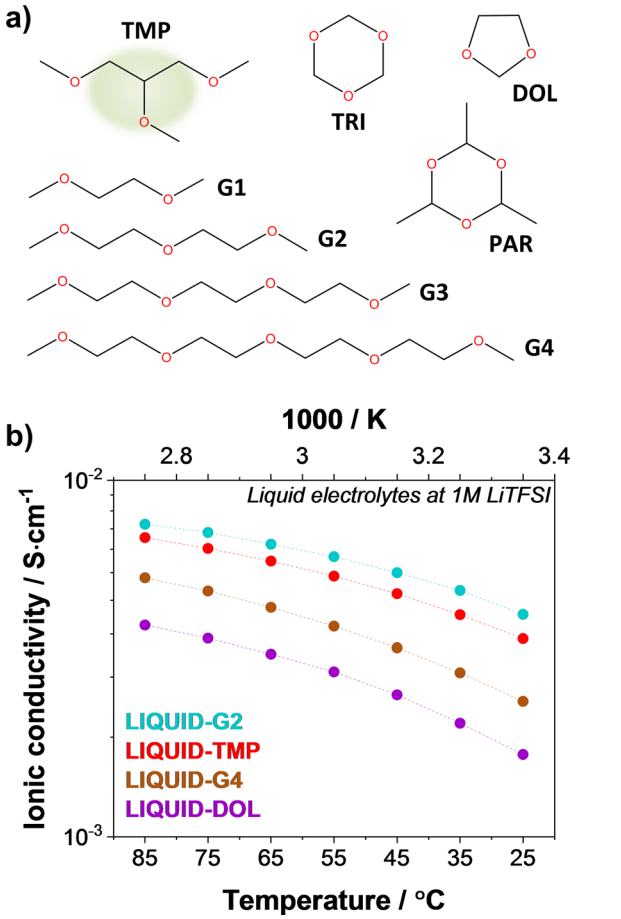

Fig. 1 (a) Chemical structures of most common ether based molecules compared to 1,2,3-trimethoxypropane (TMP): dimethoxyethane (G1), diethylene glycol dimethyl ether (G2), triethylene glycol dimethyl ether (G3), tetraethylene glycol dimethyl ether (G4), 1,3,5-trioxane (TRI), 1,3-dioxolane (DOL) and paraldehyde (PAR); and (b) ionic conductivity at different temperatures of four aprotic liquid electrolyte systems at 1 M LiTFSI.

Experimental

All material preparation and cells assemblies were carried out inside an argon filled glovebox with levels of H_2O < 0.01 ppm and O_2 < 0.01 ppm.

Materials

TMP solvent was synthesized using 1,3-dimethoxypropan-2-ol (CAS 623-69-8) developed in a previous work[22] and methyl iodide. Synthesis details are provided in ESI.† All commercial monomers and solvents were dried by adding activated 4 Å molecular sieves (Aldrich, 4–8 mesh) to reduce water content to <20 ppm (Coulumetric Karl Fisher).

Electrolyte preparation

Liquid electrolytes. Lithium bis(trifluoromethanesulfonyl) imide (LiTFSI) was mixed with the selected solvent at 1 M concentration and stirred for 2 h. LiTFSI was previously vacuum-dried at 100 °C for 24 h.

Gel polymer electrolyte. Liquid electrolytes mixtures were mixed with the three crosslinkers (glycerol propoxylate triacrylate (TA), diethylene glycol diacrylate (DA) and poly(ethylene glycol) methyl ether acrylate (PEGA)) at different ratios (Table S2†). Mixtures were stirred for 1 h before adding DAROCUR photoinitiator at 3% w/w of monomers. Then, the solution was drop-casted on a silicon mould (⌀ 11.28 mm circular voids) and irradiated with a UV-LED lamp for 6 minutes (300–400 nm, with peak at 385 nm. Lightningcure® V3, Hamamatsu). A 3D polymeric structure trapping the selected liquid electrolyte was then obtained.

Materials characterisation

Thermal stability of the GPEs was investigated by Thermal Gravimetric Analysis (TGA) employing a TGA Q 500 (TA instruments). Samples were heated from RT to 600 °C at a heating rate of 10 °C min^{-1} under nitrogen flux of 90 mL min^{-1}. Mechanical properties of the GPEs were studied by dynamic

mechanical thermal analysis (DMTA) in a Dynamic Mechanical Analyzer, Triton 2000 DMA (Triton Technology) under compression. Circular samples of 1 cm^2 and 3–4 mm thick were used. Samples were first cooled down to −100 °C with liquid nitrogen and heated till 100 °C at a heating rate of 4 °C min^{-1} and 1.0 Hz frequency during the measurement of the mechanical modulus.

Impedance spectroscopy. Ionic conductivities were measured by electrochemical impedance spectroscopy (EIS) using an Autolab 302N Potentiostat Galvanostat coupled to a Microcell HC temperature controller. A circular ∅ 11.28 mm membrane was sandwiched between two stainless steel electrodes and sealed in a Microcell under argon atmosphere. The measurements were carried out from 85 °C to 25 °C with a 30 min dwell. Frequency range was from 0.1 MHz to 0.1 Hz and 10 mV perturbation signal was applied. Ionic conductivity of gel polymer electrolytes can be calculated following the equation:[23]

$$\sigma = \frac{1}{R_b} \cdot \frac{d}{S},$$

where σ is the ionic conductivity (S cm^{-1}), d is the thickness (cm) of the GPE, S is the area (cm^2) of electrodes in contact with the GPE and R_b (Ω) is the bulk resistance of GPE (Nyquist plot).

Battery cells preparation

Electrodes. Negative electrodes consisted of a circular thin film of lithium metal (∅ 8 mm, 120 μm thick from Rockwood Lithium (US)) deposited on top of nickel foil (∅ 11.28 mm, 20 μm thick from GoodFellow (UK)). Before use, nickel foil disks were washed in ethanol in an ultrasonic bath for 1 h and then dried at 100 °C under vacuum for 24 h. Air (O_2) electrodes were prepared by coating a gas diffusion layer (GDL from Quintech (GER)) with a slurry containing Ketjen Black 600 carbon, LITHion™ dispersion binder and anhydrous 2-propanol as previously reported.[24] The coated GDLs had an average carbon loading of 0.72 mg cm^{-2}.

Lithium symmetrical cells. The developed GPEs (∅ 11.28 mm) were sandwiched between two lithium foils and placed between two stainless steel spacers electronically isolated by a PEEK cylinder and tightened by 3 nut-bolt-insulator screws. Thickness and evenness were controlled by a Teclock© thickness gauge. This stack was then placed and tighten in a sealed container to ensure inert atmosphere during testing.

Li–O_2 batteries. Li–O_2 Swagelok cells were used and placed in specifically designed PEEK container. The GPE electrolytes (∅ 11.28 mm) were sandwiched between the negative and positive electrodes. In the case of liquid Li–O_2 cells, two glass fiber sheets – previously dried at 150 °C under vacuum for 24 h (∅ 11.28 mm, Whatman®, GF/A grade) – soaked with the liquid electrolyte mixture (200 μL) were used. The positive electrode was placed with the coated side facing the electrolyte surface and an aluminium mesh was used as current collector. Lithium metal (∅ 11.28 mm) was used in the negative electrode. This stack was then tightened in a PEEK Swagelok® cell and transferred inside a sealed PEEK container. The argon gas inside the container was then purged and replaced by oxygen gas. Discharged cathodes were disassembled in a glovebox and placed in an airtight holder and analysed using a Rigaku X-ray diffractometer (2θ = 20–65°). Match! Software was used to support identifying the different phases.

Results and discussion

In order to evaluate the ionic conductivity (σ) of our new TMP-based samples, three known ether-based liquid electrolytes (LEs) with LiTFSI at 1 M concentration were additionally prepared using diglyme (G2), tetraglyme (G4) and dioxolane (DOL) solvents. Chemical structures and key properties of molecules that are relevant to battery applications are presented in Fig. 1a and Table S1,† respectively. As shown in Fig. 1b, ionic conductivities of these liquid electrolytes – including LIQUID-TMP – are particularly high, varying between 10^{-2} and 10^{-3} S cm^{-1}. The LEs with the highest σ are: LIQUID-G2 > LIQUID-TMP > LIQUID-G4 > LIQUID-DOL. LIQUID-G2 electrolyte held the highest conductivity, in accordance with other glyme-studies.[25,26] Its isomer, LIQUID-TMP, behaves in a similar manner, and it is able to achieve σ values higher than LIQUID-G4 (3.59×10^{-3} S cm^{-1} and 2.39×10^{-3} S cm^{-1} at 25 °C, respectively). Probably, this is mostly due to the lower viscosity of the TMP and G2 solvents compared to G4.[25]

In order to elucidate further some of the electrolyte properties of the LIQUID-TMP system such as the density, ionic conductivity (σ) or lithium diffusion coefficient (D_{Li^+}); a full study has been undertaken by all-atom MD simulations. To evaluate these results comprehensibly, same study was also undertaken on the LIQUID-G2 system.

Fig. S2† shows the fits obtained for both systems as a function of temperature and salt/solvent ratio. Overall, results indicate no substantial differences between LIQUID-TMP and LIQUID-G2 electrolytes. Density (Fig. S2a and S2d†) decreased linearly with increasing temperature and salt concentration (although from salt/solvent ratio of 10, it was less stiff). As expected, the Li diffusion coefficients (Fig. S2b and S2e†) and ionic conductivities (Fig. S2c and S2f†), increased with temperature. The D_{Li^+} also increased with higher salt concentration until 17 salt/solvent ratio was attempted. Regarding ionic conductivity, it increased until 12 salt/solvent ratio. Then, higher salt concentrations lead to lower conductivity values.

Fig. 2 shows MD results of the radial distribution function (RDF) and coordination number function (CNF) for G2 and TMP solvents and Li^+ ions. Each RDF and CNF curve corresponded to one of the three oxygen of the G2 and TMP molecules (for example, G2, O02 corresponds to the second O atom of G2 molecule). Overall, the simulations indicated no substantial differences in the coordination properties of the two systems. Fig. 2a shows that G2 has three RFD peaks at 2.02 Å while TMP has two different peaks at 1.98 Å and 2.06 Å, suggesting, firstly, a different behavior of the asymmetric oxygen (–(CH)–O–CH_3) in the TMP and, secondly, a similar Li–

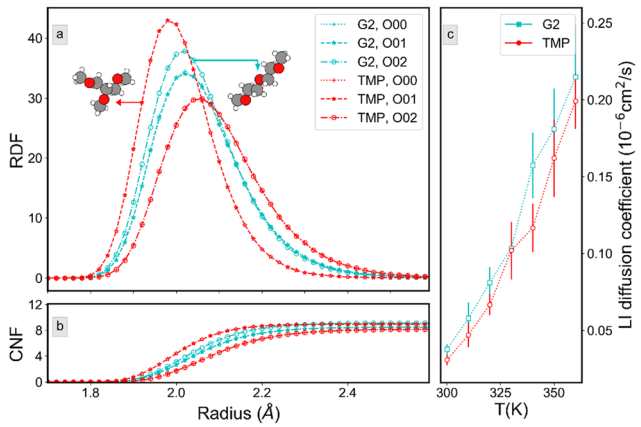

Fig. 2 Simulation results for G2 solvent (blue) and TMP solvent (red): (a) radial distribution functions for all oxygen atoms (RDF); (b) coordination number function (CNF); and (c) lithium diffusion coefficient *vs.* temperature.

O coordination for G2 and TMP. Both systems had two overlapping RDF for oxygen and the non-degenerate curve corresponds to the maximum of RDF. Fig. 2b shows the coordination numbers from numerical integration (scipy.integrate with trapezoidal rule), which were the same for the three O atoms of both TMP and G2 (8 and 9), suggesting a similar coordination of the two molecules with a Li^+ cation.

Next, gel polymer electrolytes were prepared by UV-photopolymerisation[21,24] (Fig. 3a). Liquid electrolytes (LE) using based on different aprotic ether-based solvents and LiTFSI were added to a mixture of three functional cross-linkers (TA, DA and PEGA) in the presence of 2-hydroxy-2-methylpropiophene (DAROCUR) as the radical photoinitiator. The cocktail of different acrylic oligomers was needed to tune the mechanical properties and the compatibility with the liquid electrolyte. This mixture was drop-casted on silicon mould and then UV cured. In all cases, transparent and self-standing membranes were obtained in short curing times (<1 min) (Pictures Fig. 3b). Monomer conversions were checked *via* Fourier Transform Infrared Spectroscopy (FTIR) spectra, (Fig. S3a†).[21] Conversions higher than 96% were reached, confirmed by the disappearance of the characteristic 1640–1635 cm^{-1} band associated to the C=C stretching vibration of the acrylic groups. This is due to the typical UV-curing process of photocurable acrylic resins by radical photopolymerization.

The ionic conductivity (σ) of gel polymer electrolytes with different compositions was evaluated to down select the best formulation. The compositions were varied by shifting the LE content from 50 to 90 wt%; keeping fixed the amount of tri- and di- functional acrylates at 5 wt%. Accordingly, the mono-acrylate ratio varied from 40 to 0 wt%, as shown in Table S4.† Samples were named as GPE-TMP*x* (*x* = amount of LE in wt% = 50, 70, 80, 90). After curing, all GPEs were transparent and flexible. As expected, the σ was enhanced by higher LE content (Fig. 3c). The GPE-TMP90 was self-standing but not sufficiently robust to withstand the pressure of the σ cell, hence membranes were smashed during the measurement. GPE-TMP80 was the optimised formulation chosen for further characterisation having a high σ of 2.33×10^{-3} S cm^{-1} at 25 °C, very close to its liquid counterpart (3.59×10^{-3} S cm^{-1}). The performance of the GPE-TMP80 membrane was then compared to other GPEs containing different LE, using the same GPE formulation. As shown in Fig. 4a, the GPE-TMP80 electrolyte had,

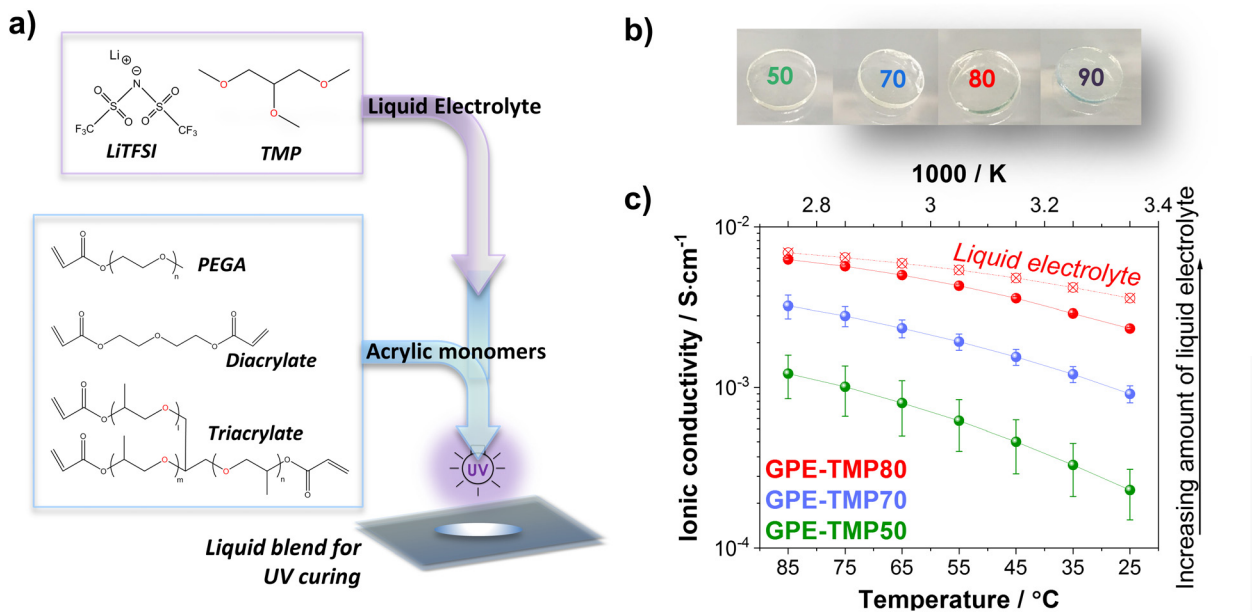

Fig. 3 (a) Schematic representation of the preparation of GPEs by UV-photopolymerisation; (b) images of the GPE membranes containing increasing amount of TMP organic plasticizer in wt%; and (c) ionic conductivity values of TMP-based solid GPEs containing 50, 70 and 80 wt% of liquid electrolyte compared to the analogue liquid electrolyte cell.

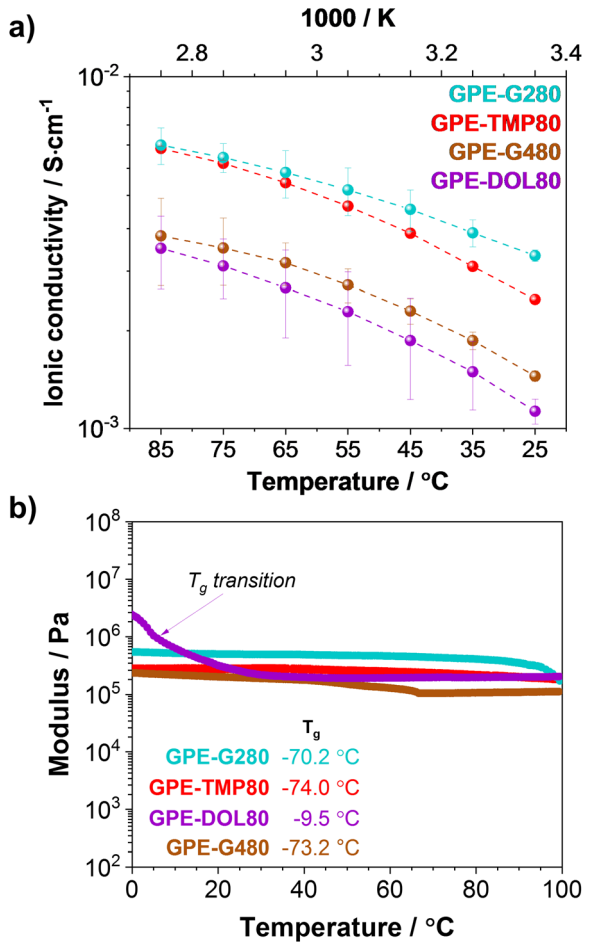

Fig. 4 GPE solid membranes containing 80 wt% plasticizers using different types of ether-based solvents: new greener trimethoxypropane (TMP), diglyme (G2), tetraglyme (G4) and dioxolane (DOL): (a) ionic conductivity values of selected GPEs at different temperatures; and (b) DMTA analysis at compression from 0 to 100 °C.

remarkably, very similar conductivities to the GPEs based on toxic glymes such as GPE-G280 membrane (2.33×10^{-3} S cm^{-1} and 3.1×10^{-3} S cm^{-1}, respectively). These conductivities were the highest achieved for all the systems investigated in this study. Furthermore, the obtained conductivities were temperature dependent and followed the well-known Arrhenius–Boltzmann model[27] (Fig. S4†).

More particularly, GPE-TMP80 showed a sharper conductivity increase than GPE-G280 indicating a higher activation energy for this membrane (0.15 eV *vs.* 0.11 eV, respectively). On cells using liquid electrolytes, this difference was smaller (0.1 *vs.* 0.09 eV for LIQUID-TMP and LIQUID-G2, respectively), and still lower than other systems (*e.g.* 0.12 eV for LIQUID-G4).

Further mechanical and thermal testing was undertaken to evaluate their feasibility as solid electrolyte battery materials during operation. Mechanical stability (dynamic mechanical thermal analysis (DMTA) at compression mode) of optimised membranes (GPE80x) are presented in Fig. 4b.

Similar to other crosslinked UV-acrylate-based systems,[28,29] the storage modulus of these samples showed values in between 10^5–10^6 Pa without significant variations across a full range of temperatures (0 to 100 °C). GPE-DOL80 presented a shoulder between 0 and 20 °C, in which the modulus decreased one order of magnitude from 10^7 Pa. This maximum is associated to its glass transition temperature (T_g = −9.5 °C). The rest of the samples presented much lower T_g, around −72 °C. DMTA was also carried out on other GPE-TMP based membranes (Fig. S3b†), showing that the storage modulus increased at higher polymer ratios. Thermal stability was also evaluated by TGA. Fig. S3c† shows TGA of the GPE-TMP based electrolytes. Overall, they showed two areas of degradation. The first (75–300 °C) was associated with the loss of solvent (more prominent in samples with higher amount of LE, *i.e.* GPE-80TMP). The second, initiated around 275 °C, was associated with the degradation of the polymeric network. Gel electrolytes containing different solvents for LE were also evaluated (Fig. S3d†) and the two-step degradation mechanism was also observed. However, significant variations on the first were detected, depending on the volatility of the solvent selected in the LE (Table S1†).

Overall, TMP-based liquid electrolytes and GPEs showed comparable ionic conductivity values to its toxic isomer (G2) or the popular G4 glyme. They were also thermal and mechanical stable materials at battery operational temperatures (from RT to ~70 °C). Electrolytes containing TMP, G2 and G4 as solvents were further investigated and compared in lithium battery cells.

Electrochemical characterisation and battery performance of TMP liquid and GPE electrolytes

Evolution of impedance at open circuit potential (OCV) through Nyquist plots was firstly evaluated for both liquid and gel electrolytes (Fig. S5a†). Lithium symmetrical cells were used for this purposed (Fig. S5b†). As displayed in Fig. S5c and S5d,† the impedance of the cells increased in all cases between the cells assembly and up to 50 h resting time at OCV at 25 °C. This increase was more significant for the cells using TMP-based electrolyte, in which the resistance increased during the first ~5 h, and then decreased reversibly by several orders of magnitude after >5–10 h. These changes in the resistance were attributed to the formation of insulating species at the electrolyte/electrode surface, as credited in other works.[30,31]

Liquid cells using TMP showed a stationary condition after 10 h, compared to the 46 h for the ones with LIQUID-G4 and 50 h for LIQUID-G2. On the other hand, gel polymer electrolytes showed this condition after 36, 34, and 38 h for cells using GPE-TMP80, GPE-G480 and GPE-G280, respectively. Fig. S6† reflects the impact of these pre-conditioning times during lithium platting/stripping 1 h cycles at different rates, varying from ±0.01 to ±1 mA cm^{-2}. When compared to a standard conditioning time fixed at 3 h, the long-time-conditioned samples showed a higher polarization, being more significant at higher current rates for both liquid and gel-based electrolyte cells. This could be explained by the fact that higher impedances translate in higher resistances for the ions at the inter-

face, lowering the mobility/diffusion and, therefore, increasing the polarization. A study from Häcker *et al.*,[30] revealed that the Nyquist spectra for a symmetric Mg/Mg cell showed a significant increase of impedance during the first 50 h after cell assembly at OCV, but then decreased remarkably by several orders of magnitude after the cells were cycled at a fixed current. By this galvanostatic polarisation, they were able to eliminate the adsorption layer formed by electrolyte species on the electrode surface that remained inactive during OCV. This would probably explain the behaviour of our 3 h conditioned cells during cycling, in which the initial impedance was much lower than the stabilised cells. Hence, the potential adsorption layer was smaller and easier to eliminate during cycling, translating in much lower overpotential during the platting/stripping of the lithium. Due to these results, a fixed 3 h conditioning was established prior to all testing.

Fig. S7† show the evolution of polarisation potentials under dynamic current rates at ±0.01, ±0.1, ±0.2, ±0.5 and ±0.8 mA cm^{-2} of lithium symmetrical cells containing liquid and GPE electrolytes based on TMP, G2 and G4 solvents, respectively. For each current density, the cells were cycled three times, held two hours per cycle. Cell polarisation potentials of the three systems (TMP, G2 and G4) were very similar up to ±0.5 mA cm^{-2} and ±0.8 mA cm^{-2} for cells using liquid and GPE electrolytes, respectively. Cells using TMP-based electrolytes displayed higher overpotentials than G2- and G4-based electrolytes, however, these were still low (≤0.6 V). Remarkably, cells using GPE-TMP80 were able to lower the polarisation potentials significantly when compared to the cells with LIQUID-TMP electrolyte. Overall, the use of gel polymer electrolytes containing TMP solvent improved the polarization potentials at high current rates in lithium symmetrical cells. At lower rates, cells with TMP-based electrolytes revealed a comparable performance to cells using more toxic electrolytes.

Furthermore, long cycling on lithium symmetrical cells at a fixed current rate was also investigated in order to evaluate the long-term stability of our GPEs.

Samples were cycled at ±0.1 mA cm^{-2} (1 h dwell) at 25 °C for about 250 hours, cut-off potential of ±0.6 V and 3 h conditioning at OCV (Fig. 5). At these cycling conditions, all cells showed an initial increase in overpotential, specially the one with TMP-based electrolytes (±0.5 V for GPE-80TMP and ±0.4 V

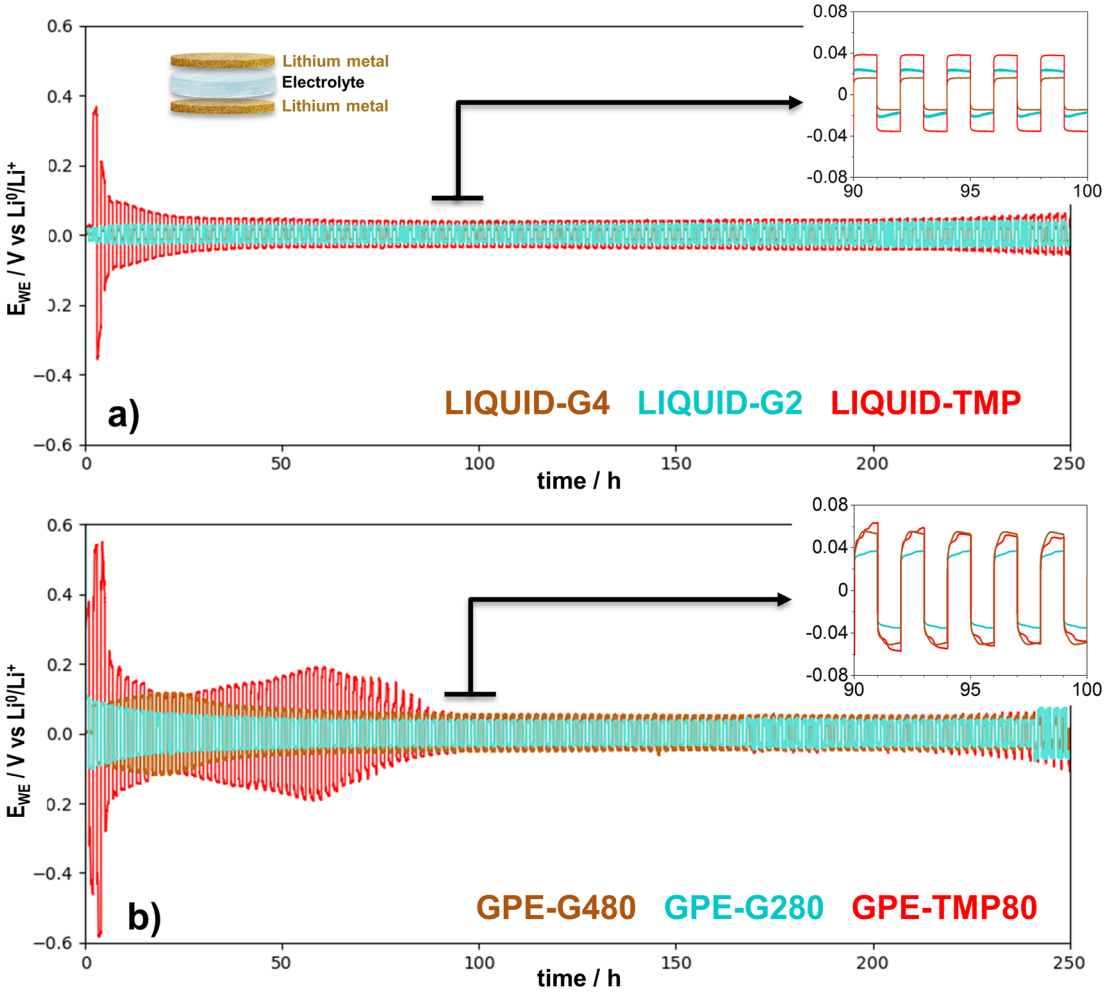

Fig. 5 Long cycling on lithium symmetrical cells at 0.1 mA cm^{-2} of (a) liquid electrolytes and (b) gel polymer electrolytes.

for LIQUID-TMP). However, cells were able to bounce back to a much lower and steady potential for the rest of the cycling. In the case of cells using GPEs (Fig. 5b), the overpotentials were observed between ±0.04–0.05 V for more than 150 h. Cells with GPE-G280 electrolyte showed the lowest overpotentials. In cells using liquid electrolytes (Fig. 5a), the overpotentials remained below ±0.04 V, standing out the cell using LIQUID-G4 electrolyte (±0.015 V). All in all, TMP-based electrolytes, including both liquid and GPE electrolytes, were able to give a comparable performance to G2- and G4-based electrolytes. It is worth noting that ether-based plasticizers, specially G2 and G4, are the most popular solvents to reduce potentials at the working lithium metal anode.[8,9,32] Hence, TMP would also belong to this high-performance-group.

To further evaluate these electrolytes, Swagelok® Li–O_2 batteries were prepared (Fig. 6a). Two types of galvanostatic discharge/charge tests at ±0.1 mA cm^{-2} and 25 °C were undertaken. On the first one, Li–O_2 cells were cycled with cut-off potentials of 2 V (discharge) and 4.6 V (charge) to determine their absolute discharge/charge capacities. On the second one, samples were cycled with limited capacity (0.2 mA h cm^{-2}) to determine their capacity retention. Tests were started after 3 h conditioning at OCV.

Firstly, cells were fully discharged and charged. As shown in Fig. S8b,† the highest absolute discharge capacity observed for GPE-based cells belonged to GPE-TMP80 (2.75 mA h cm^{-2}), followed by GPE-G280 and GPE-G480 (2.34 and 2.09 mA h cm^{-2}, respectively). In addition, liquid electrolyte counterparts were also evaluated for comparison (Fig. S8a†). The highest discharge capacity was achieved by the cell using LIQUID-G2 electrolyte (3.09 mA h cm^{-2}). Cells using LIQUID-TMP and LIQUID-G4 electrolytes showed high capacities, but lower than the one observed for cells using LIQUID-G2 (2.50 and 1.90 mA h cm^{-2}, respectively).

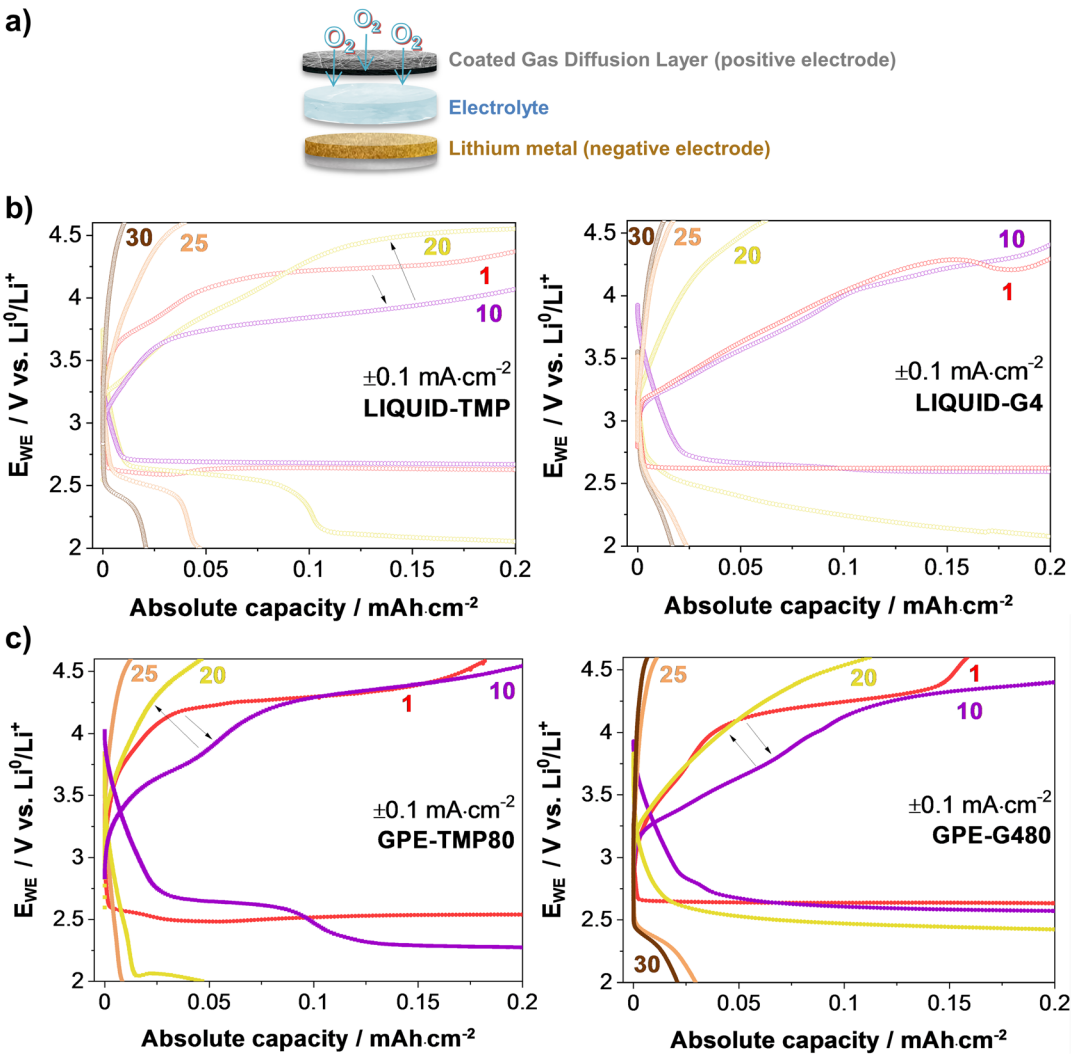

Fig. 6 (a) Scheme of Swagelok Li–O_2 configuration. (b) Discharge–charge cycling profiles of Li–O_2 cells using liquid electrolytes (LIQUID-TMP and LIQUID-G4); and (c) discharge–charge cycling profiles of Li–O_2 cells using gel electrolytes (GPE-TMP80 and GPE-G480). Only selected curves are shown, and numbers in the plots indicate number of cycle.

Interestingly, TMP and G4 electrolyte-based cells enhanced capacities by the use of gel polymer electrolytes. This behavior has been also observed on a previous work using G4 as plasticizer.[24]

Relative mass capacities (based on carbon mass) for discharge were also calculated, being as high as 3819, 3250 and 2903 mA h g^{-1} for cells using GPE-TMP80, GPE-G280 and GPE-G480 solid electrolytes, respectively. The good performance of G2 glyme electrolyte-based cells comes as no surprise. Despite the major popularity of G4 plasticizer, works in literature have proven that Li–O_2 cells with G2-based electrolytes have higher capacity and, even, higher stability during cycling,[9,14,15,32] due, amongst other reasons, to the lower stability of longer glymes[8] and their higher viscosity. Overall, TMP electrolyte-based cells displayed capacities as good as the one using toxic glymes, especially when GPE electrolytes are used.

After first full discharge, X-ray powder diffraction (XRD) patterns were obtained from the positive electrodes in order to confirm the formation of crystalline lithium peroxide, Li_2O_2, main discharge product expected in aprotic Li–O_2 cells ($2Li + O_2 + 2e^- \rightarrow Li_2O_2$).[5] Discharged cathodes of liquid cells using TMP, G2 and G4 based electrolytes were compared to a pristine cathode and reference Li_2O_2 patterns, as shown in Fig. S9a.† All of them, showed the peaks matching Li_2O_2 pattern. However, on the XRD pattern of the electrode collected from cells using TMP-based electrolyte, other peaks were clearly observed. To have a deeper insight, other components which are commonly known unwanted side products, were also analyzed as additional references: lithium carbonate (Li_2CO_3), lithium fluoride (LiF) and lithium oxide (Li_2O) (Fig. S9b†). As shown in Fig. S9b† and according to phase finding function on Match! software, on diffractogram coming from TMP-based cell electrode, crystalline peaks of both LiOH and Li_2O_2 were identified. One explanation to explain the presence of LiOH, could be that TMP promotes the formation of amorphous Li_2O_2 – or other lithium oxides – (invisible to XRD), that could react with water and form crystalline LiOH ($Li_2O_2 + H_2O \rightarrow 2LiOH + H_2O_2$).[33] Other explanation could be related to the presence of H^+ (coming from the degraded TMP or the presence of traces of water in the electrolyte), that can trigger the formation of disk-shaped LiOH *via* the unstable lithium superoxide (LiO_2).[8,34,35] In both scenarios, presence of water plays an important role. This finding should be strongly considered in future works to optimize TMP synthesis and drying.

Regarding the capacity-limited cycle performance, Fig. 6 shows the cycling curves for both liquid electrolyte and GPE-based Li–O_2 cells using TMP and G4 as plasticizers. Overall, cells using TMP (both liquid electrolyte and GPE), behaved in a similar manner to G4-based cells: similar capacities and similar number of cycles were observed. Liquid electrolyte-based cells lasted up to 30 cycles (25% capacity retention at this point). Regarding gel electrolyte based cells, cells using GPE-TMP80 started to decay (Q_{dis} < 0.2 mA h cm^{-2}) on cycle 15th, whereas the ones with GPE-G480 did so from cycle 20th. Nonetheless, the capacity retention observed was below 25% on cycle 20th for cells using GPE-TMP80 and on cycle 22nd for cells using GPE-G480, meaning the sudden decay of the G4 cell. In addition, it is worth pointing out the behavior of the cells during charge. Unexpectedly, the overpotential observed during charge improved from cycle 1 to cycle 10 in the case of LIQUID-TMP and both GPEs based electrolyte cells (GPE-TMP80 and GPE-G480). This behavior is still under investigation (out of the scope of this work), but it might be linked to the shape and/or nature of the discharge products obtained on the first cycles. Also, the authors recommend to potential future works based on TMP that cyclability performance in Li–O_2 could be greatly improve – for instance – by the use of a redox mediator, as proven in other works.[36,37] Overall, cells with TMP-based electrolytes exhibited a more moderated decay of capacity than cells using G4-based electrolytes, and similar cyclability was observed for both liquid and gel polymer electrolyte cells. Hence, these findings would confirm the capability of using TMP as the solvent or plasticizer in electrolytes for Li–O_2 cells.

Conclusions

The potential of TMP as a biobased and low toxicity alternative to currently used glymes as solvent/plasticizer in electrolytes for batteries, has been evaluated for the first time. Firstly, the ability of TMP to dissolve and conduct Li^+ ions has been demonstrated and compared to other ether-based electrolytes. Furthermore, and beyond liquid electrolytes, a robust and high-performance UV-cured gel polymer electrolyte system has been designed and evaluated to improve the overall safety of Li–O_2 batteries. GPEs based on TMP plasticizer showed a striking ionic conductivity of 2.33×10^{-3} S cm^{-1} at 25 °C, very close to its liquid electrolyte counterpart (3.59×10^{-3} S cm^{-1}). Importantly, GPEs based on TMP presented a conductivity as good as its toxic isomer G2-based GPE. These transparent and self-standing GPEs also demonstrated thermal and mechanical stability at battery operational conditions. Interestingly gel polymer electrolytes enhanced the potential of TMP-based cells to lower polarisation at high rates (up to ±2 mA cm^{-2}) on symmetrical lithium cells. At lower rates, Li symmetrical cells using TMP-based electrolytes revealed a comparable performance to cells using G2 or G4-based electrolytes. When used in Li–O_2 cells, GPEs based on TMP showed higher discharge capacities (2.75 mA h cm^{-2}) and very similar cycling behavior than cells using popular G4 glyme based electrolyte. Hence, the results shown in this work demonstrate the potential of the biobased TMP to be used as a solvent or plasticizer in battery electrolytes. TMP represents a good alternative to the use of toxic glymes (*i.e.* tetraglyme or diglyme), very popular solvents used in electrolytes for Li–O_2 batteries. Furthermore, and beyond lithium–O_2 cells, this greener solvent could be used in other battery technologies. Additionally, TMP is just one of many possible branched glymes that can be derived from glycerol and there are opportunities to further optimize its molecular structure for Li–O_2 battery applications.

Author contributions

The manuscript was written through contributions of all authors. M. A. T. performed the experiments, analyzed the data and wrote the manuscript. L. C. and D. M. supervised and contributed to the conception and design of the work, analysis of data and review of the manuscript. A. G. contributed to the analysis of data and testing. S. Q. synthetized and characterized TMP solvent. J. E. B. reviewed the manuscript and contributed to data analysis. M. D. G. designed and carried out the MD simulations and K. G. contributed to the MD design and supervision. All authors have given approval to the final version of the manuscript.

Conflicts of interest

There are no conflicts to declare.

Acknowledgements

This work was supported by the European Commissioń s funded Marie Skłodowska-Curie project POLYTE-EID (Project No. 765828). M. D. G. acknowledges Nicholas Michelarakis and Agilio Padua for fruitful discussions and Klanik SA. In addition, M. A. T. would like to thank Dr Gregorio Guzmán-González for his invaluable discussions about Li^+ chelation. The manuscript was written through contributions of all authors that have given approval to the final version of the Letter.

Notes and references

1 T. M. Gür, *Energy Environ. Sci.*, 2018, **11**, 2696–2767.
2 X. Zeng, M. Li, D. Abd El-Hady, W. Alshitari, A. S. Al-Bogami, J. Lu and K. Amine, *Adv. Energy Mater.*, 2019, **9**, 1–25.
3 M. M. Titirici, *Adv. Energy Mater.*, 2021, **2003700**, 1–11.
4 C. Sun, *Adv. Mater. Lett.*, 2018, **9**, 336–344.
5 W.-J. Kwak, Rosy, D. Sharon, C. Xia, H. Kim, L. R. Johnson, P. G. Bruce, L. F. Nazar, Y.-K. Sun, A. A. Frimer, M. Noked, S. A. Freunberger and D. Aurbach, *Chem. Rev.*, 2020, **120**, 6626–6683.
6 L. Grande, E. Paillard, J. Hassoun, J. B. Park, Y. J. Lee, Y. K. Sun, S. Passerini and B. Scrosati, *Adv. Mater.*, 2015, **27**, 784–800.
7 S. Tang and H. Zhao, *RSC Adv.*, 2014, **4**, 11251–11287.
8 J. Lai, Y. Xing, N. Chen, L. Li, F. Wu and R. Chen, *Angew. Chem., Int. Ed.*, 2020, **59**, 2974–2997.
9 S. Choudhury, Z. Tu, A. Nijamudheen, M. J. Zachman, S. Stalin, Y. Deng, Q. Zhao, D. Vu, L. F. Kourkoutis, J. L. Mendoza-Cortes and L. A. Archer, *Nat. Commun.*, 2019, **10**, 1–11.
10 M. Sutter, W. Dayoub, E. Métay, Y. Raoul and M. Lemaire, *ChemCatChem*, 2013, **5**, 2893–2904.
11 M. Sutter, L. Pehlivan, R. Lafon, W. Dayoub, Y. Raoul, E. Métay and M. Lemaire, *Green Chem.*, 2013, **15**, 3020–3026.
12 B. S. Flowers, M. S. Mittenthal, A. H. Jenkins, D. A. Wallace, J. W. Whitley, G. P. Dennis, M. Wang, C. H. Turner, V. N. Emel'Yanenko, S. P. Verevkin and J. E. Bara, *ACS Sustainable Chem. Eng.*, 2017, **5**, 911–921.
13 C. M. Alder, J. D. Hayler, R. K. Henderson, A. M. Redman, L. Shukla, L. E. Shuster and H. F. Sneddon, *Green Chem.*, 2016, **18**, 3879–3890.
14 D. Hirshberg, D. Sharon, M. Afri, R. Lavi, A. A. Frimer, N. Metoki, N. Eliaz, W. J. Kwak, Y. K. Sun and D. Aurbach, *ACS Appl. Mater. Interfaces*, 2018, **10**, 10860–10869.
15 G. Horwitz, E. J. Calvo, L. P. Méndez De Leo and E. De La Llave, *Phys. Chem. Chem. Phys.*, 2020, **22**, 16615–16623.
16 J. Gąsiorek, *Przem. Chem.*, 2015, **94**, 166–168.
17 J. S. Chang, Y. Da Lee, L. C. S. Chou, T. R. Ling and T. C. Chou, *Ind. Eng. Chem. Res.*, 2012, **51**, 655–661.
18 G. D. Barbosa, J. E. Bara and C. H. Turner, *Phys. Chem. Chem. Phys.*, 2022, **24**, 9459–9466.
19 K. Chen, D.-Y. Yang, G. Huang and X.-B. Zhang, *Acc. Chem. Res.*, 2021, **54**, 632–641.
20 Q. Wang, H. Wang, J. Wu, M. Zhou, W. Liu and H. Zhou, *Nano Energy*, 2020, **80**, 105516.
21 V. Vijayakumar, B. Anothumakkool, S. Kurungot, M. Winter and J. R. Nair, *Energy Environ. Sci.*, 2021, **14**, 2708–2788.
22 S. Qian, X. Liu, G. P. Dennis, C. H. Turner and J. E. Bara, *Fluid Phase Equilib.*, 2020, **521**, 112718.
23 X. Qian, N. Gu, Z. Cheng, X. Yang, E. Wang and S. Dong, *J. Solid State Electrochem.*, 2001, **6**, 8–15.
24 M. Alvarez Tirado, L. Castro, G. Guzmán-González, L. Porcarelli and D. Mecerreyes, *ACS Appl. Energy Mater.*, 2021, **4**, 295–302.
25 M. Tang, J.-C. Chang, S. R. Kumar and S. J. Lue, *Energy*, 2019, **187**, 115926.
26 K. Deng, Q. Zeng, D. Wang, Z. Liu, Z. Qiu, Y. Zhang, M. Xiao and Y. Meng, *J. Mater. Chem. A*, 2020, **8**, 1557–1577.
27 S. B. Aziz, T. J. Woo, M. F. Z. Kadir and H. M. Ahmed, *J. Sci.: Adv. Mater. Devices*, 2018, **3**, 1–17.
28 M. W. Logan, S. Langevin, B. Tan, A. W. Freeman, C. Hoffman, D. B. Trigg and K. Gerasopoulos, *J. Mater. Chem. A*, 2020, **8**, 8485–8495.
29 L. Porcarelli, A. S. Shaplov, F. Bella, J. R. Nair, D. Mecerreyes and C. Gerbaldi, *ACS Energy Lett.*, 2016, **1**, 678–682.
30 J. Häcker, C. Danner, B. Sievert, I. Biswas, Z. Zhao-Karger, N. Wagner and K. A. Friedrich, *Electrochim. Acta*, 2020, **338**, 135787.
31 Z. Zhao-Karger, R. Liu, W. Dai, Z. Li, T. Diemant, B. P. Vinayan, C. Bonatto Minella, X. Yu, A. Manthiram, R. J. Behm, M. Ruben and M. Fichtner, *ACS Energy Lett.*, 2018, **3**, 2005–2013.
32 D. Sharon, D. Hirshberg, M. Afri, A. A. Frimer and D. Aurbach, *Chem. Commun.*, 2017, **53**, 3269–3272.

33 D. Sharon, D. Hirsberg, M. Salama, M. Afri, A. A. Frimer, M. Noked, W. Kwak, Y. K. Sun and D. Aurbach, *ACS Appl. Mater. Interfaces*, 2016, **8**, 5300–5307.
34 T. Liu, M. Leskes, W. Yu, A. J. Moore, L. Zhou, P. M. Bayley, G. Kim and C. P. Grey, *Science*, 2015, **350**, 530–533.
35 Z. Li, S. Ganapathy, Y. Xu, J. R. Heringa, Q. Zhu, W. Chen and M. Wagemaker, *Chem. Mater.*, 2017, **29**, 1577–1586.
36 B. J. Bergner, A. Schürmann, K. Peppler, A. Garsuch and J. Janek, *J. Am. Chem. Soc.*, 2014, **136**, 15054–15064.
37 X. Liu, X. Xin, L. Shen, Z. Gu, J. Wu and X. Yao, *ACS Appl. Energy Mater.*, 2021, **4**, 3975–3982.